Journal of Ovarian Research

RESEARCH

Open Access

Drug-free in vitro activation combined with ADSCs-derived exosomes restores ovarian function of rats with premature ovarian insufficiency

Qian Li[1,2*†], Zhiqiang Zhang[2†], Wenxin Shi[2], Zhongkang Li[2], Yanlai Xiao[2], Jingkun Zhang[2*] and Xianghua Huang[2*]

Abstract

Background Drug-free in vitro activation (IVA) is a new protocol to activate residual dormant follicles for fertility restoration in patients with premature ovarian insufficiency (POI). However, several deficiencies have reduced its clinical efficacy rate. Our previous studies have confirmed that the combination of adipose-derived stem cells (ADSCs) and drug-free IVA can improve the effectiveness of drug-free IVA and restore ovarian function of rats with POI. Increasing evidence has demonstrated that mesenchymal stem cell-derived exosomes have similar therapeutic effects as their source cells. Here, we performed a preclinical study to evaluate the therapeutic effects of ADSCs-derived exosomes (ADSCs-Exos) combined with drug-free IVA in the POI rats and the mechanism in restoring ovarian function.

Results In vivo, the effects of ADSCs-Exos were comparable to those of ADSCs, and the ADSCs-Exos combined with drug-free IVA was better than ADSCs-Exos alone therapy in promoting follicular development. Moreover, transplantation of ADSCs/ADSCs-Exos lead to up-regulation of BCL-2 expression and down-regulation of the expression of Bax and Cleaved Caspase-3, thus reducing the apoptosis of chemotherapy-induced follicle cells, and further promoting the development of the follicles and rescuing ovarian function in POI-damaged ovary. In vitro, ovarian fragmentation could activate follicular growth and development, and in combination with ADSCs-Exos could prevent the loss of follicles, promote follicular proliferation and inhibit apoptosis.

Conclusions ADSCs-Exos combined drug-free IVA had remarkable therapeutic effects in restoring ovarian function of POI rats, and markedly promoted follicular development and inhibited apoptosis of ovarian cells in vitro. Our study confirmed that the combination therapy might be a promising and effective treatment for POI.

Keywords Drug-free in vitro activation, Adipose-derived stem cells, Exosomes, Premature ovarian insufficiency, In vitro ovarian culture, Apoptosis

†Qian Li and Zhiqiang Zhang contributed equally.

*Correspondence:
Qian Li
qiuyeyuhan123@163.com
Jingkun Zhang
zhangjingk110110@163.com
Xianghua Huang
huangxh2003@163.com
Full list of author information is available at the end of the article

Background

POI refers to the menstrual disorders in women younger than 40 years, which is characterized by follicle dysfunction, decline in ovarian function and hormone imbalance [1]. Although residual follicles can be detected in several patients, they are dormant and cannot be activated by traditional methods. Therefore, egg donation is the only option for women with fertility needs [2]. IVA is a new protocol to activate residual dormant follicles by ovarian fragmentation disrupting Hippo signaling, followed by phosphatase and tensin homolog (PTEN) enzyme inhibitor or phosphatidylinositol-3-kinase (PI3K) activator, which enable patients to have their own biological children. Since the first clinical application in 2013, several live births have been reported [3, 4]. However, the effectiveness of traditional IVA is significantly reduced due to the secondary surgical trauma in a short period of time, follicle loss and pharmacological toxicity during ovarian culture in vitro. Therefore, a simplified drug-free IVA was proposed in 2018 [5], which only requires one operation to transplant fragmented ovaries in situ, without the need for pharmacological methods for in vitro culture, resulting in less invasive and higher efficiency [6]. However, the clinical effectiveness is reduced by the massive loss of primordial follicles and failure to improve age-related oocyte quality [4, 6], so further research is needed to ameliorate these deficits.

One of the effective treatment strategy for ovarian failure is the application of ADSCs, which possess the basic characteristic of mesenchymal stem cell (MSCs) and have a wide range of sources and multipotent characteristics [7–12]. Our previous studies confirmed that the combination of ADSCs and drug-free IVA could promote early graft angiogenesis and reduce ischemic injury of follicles, thus restoring ovarian function and improving the effectiveness of drug-free IVA to a certain extent [13]. Increasing evidence in recent years has demonstrated that the therapeutic effect of MSCs is mainly derived from their paracrine function and mediated by their derived exosomes (Exos) [14–17]. Exos are a class of tiny bilayer extracellular vesicles with a diameter of 30–150 nm, which can play a key role in promoting tissue and organ repair and immune metabolism regulation by delivering various important substances such as RNA, proteins and lipids [18, 19]. Exos derived from MSCs (MSCs-Exos) have similar therapeutic effects as their source cells [20], and are expected to become a new therapeutic strategy due to their more stable properties, amenable to standardization of preparation, convenient preservation and transportation, and no risk of tumorization and embolization [21–23].

In this study, we further evaluated whether ADSCs-Exos combined with drug-free IVA could restore ovarian function of POI rats and compared whether combined therapy was more effective than ADSCs/ADSCs-Exos alone. To test this hypothesis, we conducted in vivo as well as in vitro experiments to investigate the feasibility of ADSCs-Exos as a cell-free alternative to ADSCs for the treatment of POI.

Methods

Isolation and identification of ADSCs-Exos

The primary ADSCs were isolated, cultured, and characterized as reported in our previous study [13]. Exos were obtained from the supernatant of ADSCs at the third to fifth passages by ultracentrifugation method [24]. In brief, ADSCs at 70–80% confluence were cultured with DMEM/F12 (Sigma, USA) deprived of fetal bovine serum (FBS) for 72 h and the supernatant was collected. Subsequently, the centrifu- gation of the collected medium was performed at 2000×g for 15 min and 10,000×g for 30 min at 4℃ to remove cells, cellular debris and apoptotic bodies. The supernatant was then filtered through 0.22 μm needle filter (Millipore, USA) followed by ultracentrifugation at 120,000×g for 90 min at 4℃, the precipitates were resuspended in PBS and the above ultracentrifugation process was repeated for another time. The ADSCs-Exos enriched pellets were dissolved in 160 μl PBS (Servicebio, China) and stored at -80℃ for the subsequent experiments. The morphology and size distribution of the ADSCs-Exos were identified by transmission electron microscopy (TEM, HITACHI H-7650, Japan) and nanoparticle tracking analysis (NTA, Nanosight NS300, Malvern Instruments). The exosomal protein concentration and specific biochemical markers (CD63, CD9, TSG101 and GM130) were measured by bicinchoninic acid (BCA) protein assay kit (Thermo Fisher, USA) and Western blot analysis.

Establishment of POI rat model and experimental animals

Female specific pathogen-free (SPF) Sprague–Dawley (SD) rats (15 days and 8–10 weeks old) were obtained from HFK Bioscience Co. (Beijing, China), and all experimental protocols were conducted in accordance with the Ethics Committee of the Affiliated Hospital of Chengde Medical University (CYCYLL2023713).

Our purpose of dividing the study into seven groups was to investigate whether ADSCs-Exos treatment produced the same therapeutic effect as ADSCs treatment, and to further compare whether combined therapy might have better treatment outcomes than ovarian fragments/ADSCs/ADSCs-Exos therapy alone group. The establishment of POI model (cyclophosphamide, Sigma, USA; the first dose was 50 mg/kg/ intraperitoneal injection and 8 mg/kg/day for the following 14 consecutive days) was carried out following our previously reported

protocol [13]. By contrast, in the control group, the same amount of saline (Servicebio, China) was administered via an intraperitoneal injection. One day after the final administration, sixty rats were randomized into five different treatment groups ($n=12$, each group, schematic representation is shown in Fig. 1): (1) control group; (2) POI group (intra-bursa injection with 100 µl PBS for each rat, 50 µl on each side); (3) fragment-alone group [intraovarian cystic orthotopic transplantation of ovarian fragments ($1\times1\times1$ mm^3)]; (4) fragment-ADSCs group [intraovarian cystic orthotopic transplantation of ovarian fragments combined with ADSCs (6×10^6 ADSCs in 100 µl PBS for each rat, 50 µl per side)]; (5) ADSCs-treated group (intra-bursa injection with 100 µl PBS containing 6×10^6 ADSCs for each rat, 50 µl per side). To further explore whether the underlying mechanism of action involves paracrine secretion, we investigate the effects of ADSCs-Exos on the chemotherapy-induced ovarian damage. Twenty-four female POI rats were randomly divided into two different treatment groups: (6) ADSCs-Exos-treated group (intra-bursa injection with 100 µl PBS containing 300 µg ADSCs-Exos for each rat, 50 µl per side, repeated tail vein dosing after 48 h); (7) fragment-ADSCs-Exos group [intraovarian cystic orthotopic transplantation of ovarian fragments combined with ADSCs-Exos (300 µg ADSCs-Exos in 100 µl PBS for each rat, 50 µl per side, repeated tail vein dosing after 48 h)].

The rats in each of experimental treatment groups, bilateral 1-cm longitudinal microincisions were made to expose the bilateral ovaries (Fig. S1A). The ovaries were ligated with 6–0 dissolving suture (Shanghai Pudong Jinhuan Medical Products Co., LTD) and removed, and the avoidance of fallopian tube injury must be cared during the process. After removing the unwanted surrounding tissues, ovarian cortices were fragmented into tiny strips ($1\times1\times1$ mm^3). The fragment-alone/fragment-ADSCs /fragment-ADSCs-Exos groups were established by immediately transplanting the ovarian fragments (with or without ADSCs/ADSCs-Exos) back to the tunnel beneath the ovarian bursa after an incision of the ovary. The ADSCs-treated/ADSCs -Exos-treated groups were constructed by intra-bursa injecting ADSCs/ADSCs-Exos in 50 µl PBS in each ovary using an insulin syringe (BD, USA). At 2, and 4 weeks after transplantation, six rats from each group were euthanized and the bilateral ovaries were collected for subsequent experimentation.

Tracking of transplanted ADSCs-Exos in the ovaries

For in vivo tracking in the ovaries, the Exos were labeled with EvLINK 555 (illuTINGO, cat.EL012100210) following the instruction. Briefly, the detection liquid was added to the concentrated exocrine original liquid in the ratio of 1:30, the mixture was incubated for 30 min at room temperature protected from light, followed by using CORE400 (Millipore, USA) column chromatography at $2000\times g$ for 3 min, and the purified samples were collected and injected into the ovarian lumen of POI rats. At one week after transplantation, the paired ovaries were removed and processed for Exos localization. The ovaries were embedded in optimal cutting temperature (OCT) and serially sectioned into 6 µm in thickness, the nuclear was stained blue with DAPI (SouthernBiotech, USA), and red fluorescence signals were detected to trace the location of EvLINK 555-marked ADSC-Exos using a fluorescence microscope (Olympus, Japan).

In vitroovarian culture and analysis

Ovaries from 15-day-old SD rats were removed and cultured in 24-well transwell insert (Millipore, USA) to investigate the effect of in vitro activation combined with Exos on follicular development. The dissected ovaries were washed in Leibovitz's-15 medium (Gibco, USA) containing 10% FBS (Gibco, USA) and cultured on 0.4 µm transwell inserts with 0.3 ml culture medium in the lower chamber at 37℃ humidified atmosphere with 5% carbon dioxide for 2 and 4 days. A drop of culture medium was added to the surface of the ovary to prevent dryness and the culture solution was replaced every 2 days. The culture medium was DMEM/F12 (Gibco, USA) supplemented with 50 µg/ml ascorbic acid (Sigma, USA), 1% insulin-transferrin-sele- nium (Invitrogen, USA), 1 mg/ml BSA (Gibco, USA), 1 mg/ml AlbuMaxII (Invitro- gen, USA) as well as 1% penicillin/streptomycin (Gibco, USA). The ovaries were randomly distributed to different treatment groups ($n=5$): (1) control group (in-vitro -culture of the whole ovary); (2) fragment-alone group (in-vitro-cultured ovary was cleaved in half); (3) fragment-low-Exos group (ovary fragments co-incubated with 2 µg/ml Exos); (4) fragment-high-Exos group (ovary fragments co-incubated with 20 µg/ml Exos). After culture for 2 and 4 days, the ovaries were harvested and paraffin- embedded for subsequent analysis. Ovarian morphology and follicle counts were observed and photographed by an optical microscope (Zeiss, Germany). Expression of proliferating cells was detected by immunofluorescence staining of Ki67 using specific antibodies (1:1000, servicebio, China). Apoptosis cells were then examined by Cleaved Caspase-3 immunofluorescence staining (1:2000, CST, USA).

Analysis of ovarian morphology and follicle counts

The ovaries from the in vivo orthotopic transplantation and in vitro culture experi- ments were collected and fixed in 4% paraformaldehyde (Servicebio, China). The tissues were embedded in paraffin, sectioned into 5 µm in thickness, and then stained with Hematoxylin and Eosin

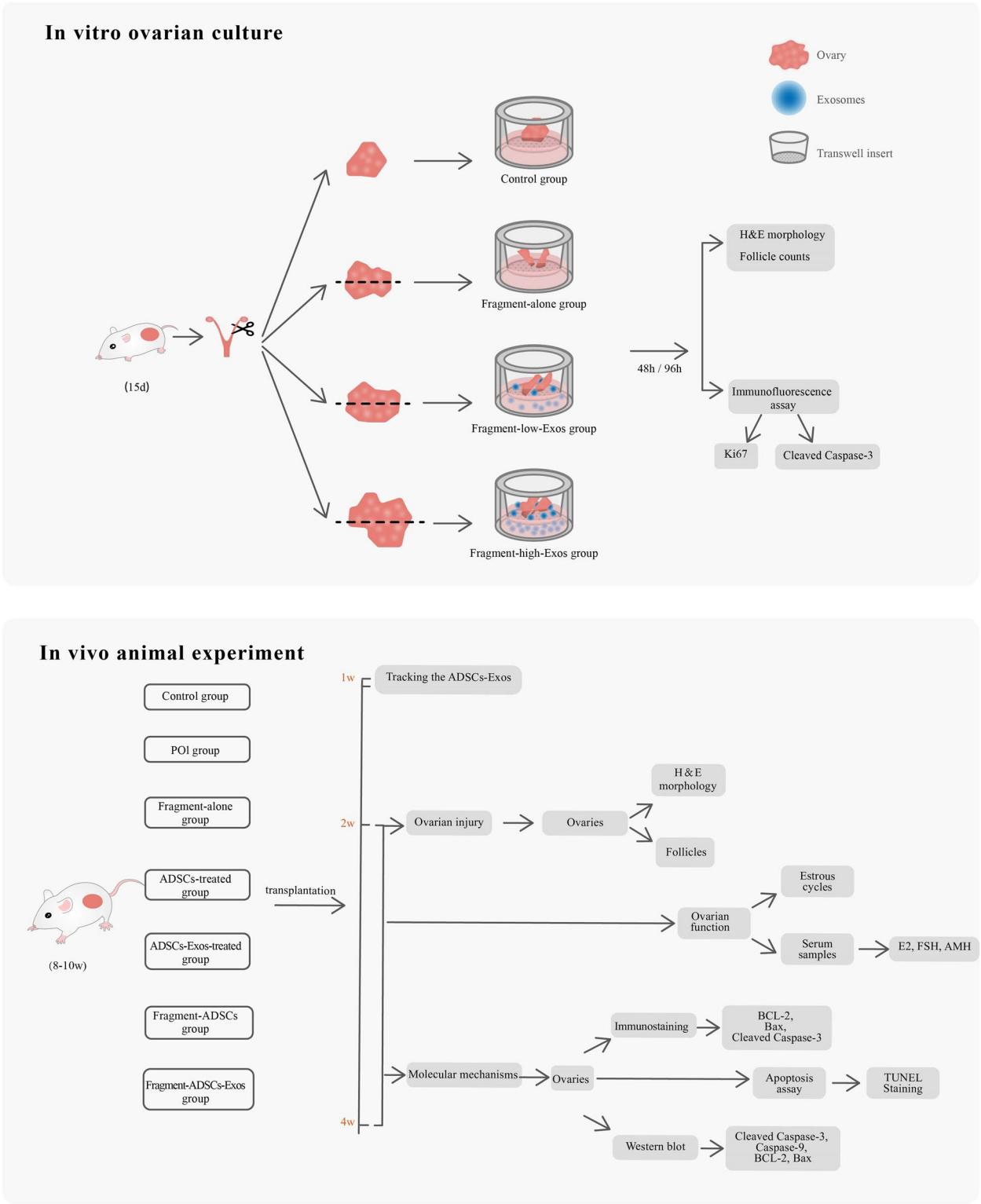

Fig. 1 Schematic diagram of experimental protocols. Schematic diagram of in vitro culture experiment and in vivo animal experiment

(HE; Servicebio, China). Ovarian morphology and follicle phenotype were observed and photographed using an optical microscope, and the counting of the follicles number at different stages (primordial, primary, secondary and antral follicles) were described as previously reported [25]. Follicles were calculated only if the oocyte had a round visible nucleus to avoid recounting.

Immunohistochemistry staining and apoptosis assay

The expression of BCL-2 and Bax proteins was investigated by immunohistochemis- try staining as previously described [13]. Briefly, the ovarian tissue sections were dewaxed to water, followed by microwave antigen retrieval, blockage for 1 h with 10% goat serum, and then incubation with primary antibody [anti-BCL-2 (1:100, Zen- bioscience, China); anti-Bax (1:100, Zen-bioscience, China)] overnight at 4℃. After washing, the sections were incubated with the corresponding secondary antibody (ZSGB-Bio, China) in 37℃ water bath for 1 h followed by staining with DAB stain- ing solution (ZSGB-Bio, China). Hematoxylin was used for nuclear counterstaining. The number of BCL-2-positive and Bax-positive areas was evaluated by counting five randomly selected fields of three nonconsecutive sections from per sample.

To further explore the effect of several treatment approaches on apoptosis of ovarian tissue, immunofluorescence staining of Cleaved Caspase-3 and TUNEL staining were carried out in all groups at 4 weeks after transplantation. For immunofluorescence staining, the paraffin-embedded tissue sections were blocked with mixed liquor (0.2% TritonX-100 and 3% goat serum in 0.1 M PBS) for 1.5 h in 37℃ water bath, and then incubated with anti-Cleaved Caspase-3 antibody (1:1000, CST, USA) and anti-Ki67 antibody (1:800, Zen-bioscience, China) overnight at 4℃. After rinsing, sections were incubated with corresponding fluorescent-conjugated secondary antibody (1:500, Abbkine, USA) at 37℃ for 1.5 h followed by DAPI counterstaining the nuclei. Pictures were captured using fluorescence microscope (Olympus, Japan) for analysis by Image J software. The TUNEL staining was conducted with the use of One Step TUNEL Apoptosis Assay Kit (Beyotime, C1088, China) according to the instruction. Briefly, the slices were incubated with proteinase K (20 μg/ml) for 30 min at 37℃ prior to staining with TUNEL detection liquid for 60 min at 37℃, protected from light. The nucleus was labeled blue with DAPI and apoptotic cells were imaged with fluorescence microscope.

Hormone assay

Blood samples from each experimental rats were harvested from orbital veins of the rats in the diestrus and the serum was frozen at -80℃ for subsequent analysis after centrifugation (4000 × g, 10 min, 4℃) using the ultracentrifuge (Hitachi Ultracentri- fuge, Japan). The concentration of serum estradiol (E_2), anti-Müllerian hormone (AMH), as well as follicle-stimulating hormone (FSH), were detected by ELISA kit (Cloud-Clone, China) according to the standard instructions. Finally, the absorbance of the sample was determined at 450 nm with the use of a microplate reader (Bio-Rad, USA).

Western blot analysis

The ovaries from the in vivo orthotopic transplantation were lysed with RIPA lysis buffer (servicebio, China) containing protease and phosphatase inhibitor mixture (servicebio, China). BCA Protein Assay (Thermo, USA) was performed to measure protein concentration. The denatured proteins were resolved by 10% or 12.5% SDS-PAGE (Biotides, China) and transferred to PVDF membranes (Millipore, USA). Following blocking for 1 h with 5% skim milk (solarbio, China), the membranes were then incubated overnight at 4℃ with corresponding primary antibody in antibody dilutions, namely, anti-BCL-2 (1:1000, Zen-bioscience, China), anti-Bax (1:1000, Zen-bioscience, China), anti-Caspase-3 (1:1000, Zenbioscience, China), anti-Cleaved Caspase-3 (1:1000, CST, USA), anti-Caspase-9 (1:1000, Zen-bioscience, China), anti-Cleaved-Caspase-9 (1:1000, Zen-bioscience, China), and anti-GADPH (1:4000, Servicebio, China). Subsequently, the membranes were incubated with corresponding secondary antibodies (anti-mouse IgG-HRP 1:10,000, anti-rabbit IgG-HRP 1:15,000, Mei5bio, China) for 1 h at room temperature. Lastly, blot signals were detected by ChemiDoc MP Imaging System (Bio-Rad, USA) for analysis using Image J software.

Statistical analysis

All statistical data were analyzed by GraphPad Prism 6.0 and numerical values with normal distribution are presented as the mean ± SD. A Student t-test, one-way analysis of variance (ANOVA) and Mann–Whitney U-test were employed for comparison of intergroup differences. $P < 0.05$ was considered as statistically significant.

Results

Identification and in vivo tracking of ADSCs-Exos

Our previous studies had described the identification of ADSCs [13]. In the present study, we successful extracted Exos from serum-free ADSCs culture supernatants by using gradient ultracentrifugation method. The representative TEM images of Exos exhibited a typical spherical-cup-like shape that was around 100 nm in diameter (Fig. S1B). The NTA analysis indicated that the average size of the particles was 121.2 nm, which was in the expected size range of Exos (Fig. S1C). The findings

of Western blot analysis revealed that the isolated Exos were positively expressed with CD9, CD63, TSG101, but did not express the negative marker GM130 (Fig. S1D). All these results indicated the successful isolation of Exos.

In our previous study, we had demonstrated distribution of the transplanted ADSCs in the interstitium of the ovaries rather than in the follicles [13]. The purpose of the present study was to trace the distribution of Exos in the ovary. The ADSCs-Exos were labeled with the fluorescent tracer dyes which were injected into the ovarian lumen. At one week after transplantation, the strong red signal was detected in the somatic cells of ovarian cortex, as shown in Fig. S1E. All these results suggested that both ADSCs and ADSCs-Exos showed specific enrichment in ovarian cortex of the damaged ovary.

ADSCs combined with drug-free IVA efficiently rescued the ovarian function through paracrine mechanism in POI rats

To access the therapeutic effects of ADSCs or ADSCs-Exos combined with drug-free IVA on ovarian function of POI rats, we established a POI rat model following our previously established method [13] and the treatment was performed as described in the flowchart (Fig. 1). HE staining indicated that markedly reduced number of follicles at each stage were observed in the POI group, as compared with the control group (Fig. 2A). In the fragment-alone group, there was an obviously increased number of growing follicles, but no changes in the number of primordial follicles. However, the number of primordial and growing follicles markedly increased in the other four treatment groups. In particular, there was the most marked increase in the number of secondary and antral follicles, in the fragment-ADSCs group and fragment-ADSCs-Exos group. The statistical analysis of follicle count also obtained the same result (Fig. 2B). At 2 weeks after treatment, although the number of primary, secondary and antral follicles in the fragment-alone group was higher than that in the POI group ($P<0.001$), there was no significant increase in the number of primordial follicles ($P>0.05$). At 4 weeks after treatment, the number of follicles at all developmental stages in the fragment-alone group increased compared with the POI group ($P<0.001$), but this increase was more pronounced in the other four treatment groups ($P<0.01$). Compared with the POI group, the ADSCs-containing-treated ($P<0.001$) and ADSCs-Exos-containing-treated groups ($P<0.001$) observed a significant increase in the number of follicles at each stage from 2 weeks after transplantation and reached normal levels by 4 weeks. From the statistical results, it could be seen that fragment-ADSCs/fragment-ADSCs-Exos-treated groups promoted secondary and antral follicular development more than ADSCs-treated/ADSCs-Exos-treated group ($P<0.05$), but no statistical difference was found between the two groups ($P>0.05$). Taken together, these results demonstrated that either the ADSCs-containing-treated groups or the ADSCs-Exos-containing-treated groups could promote follicular development and increase ovarian reserve, and that ADSCs-Exos treatment could achieve similar therapeutic effects as ADSCs treatment. Moreover, ovarian fragments combined with ADSCs/ADSCs-Exos treatment was more effective than the ADSCs/ADSCs-Exos treatment alone in promoting follicular development.

Subsequently, body weight, estrous cycle and body condition were monitored daily after treatment and compared with the POI group. Starting from 2 weeks after transplantation, the weights of rats in each treatment group were significantly increased than those of rats in the POI group ($P<0.001$), especially in the fragment-ADSCs group and fragment-ADSCs-Exos group, which showed more significant weight gain compared with the other three treatment groups (Fig. 2E, $P<0.001$). The monitoring results of estrous cycle showed that the irregular estrous cycles began to resume starting from 2 weeks after treatment, which was most pronounced at 4 weeks after treatment (Fig. 2D). The results of hormones detection indicated that at 2 weeks post-transplantation, except no changes in E_2 within the fragment-alone group (Fig. 2C, $P>0.05$), the levels of E_2, AMH and FSH gradually recovered in each treatment group, especially in the four treatment groups containing ADSCs/ADSCs-Exos ($P<0.001$). At 4 weeks after treatment, although the levels of E_2 ($P<0.001$) and AMH ($P<0.001$) were remarkably increased and the level of FSH ($P<0.001$) was remarkably decreased in the fragment-alone group, as compared with the POI group, its hormone recovery levels were still lower than those of the other four treatment groups ($P<0.05$). The aforementioned results demonstrated that all treatment groups were able to restore serum hormone and ovarian function, especially in the groups containing ADSCs/ADSCs-Exos, but there was no significant difference among the four treatment groups except body weight ($P>0.05$).

ADSCs combined with drug-free IVA efficiently reduced apoptosis of ovarian granulosa cells (GCs) in POI rats

To further explore the therapeutic mechanisms of ADSCs combined with drug-free IVA on the recovery of ovarian function, we measured the expression of apoptosis- associated molecules by immunochemistry, immunofluorescence, and Western blot. Compared with the POI group, the result of immunochemistry demonstrated that Bax-positive cells were remarkably down-regulated

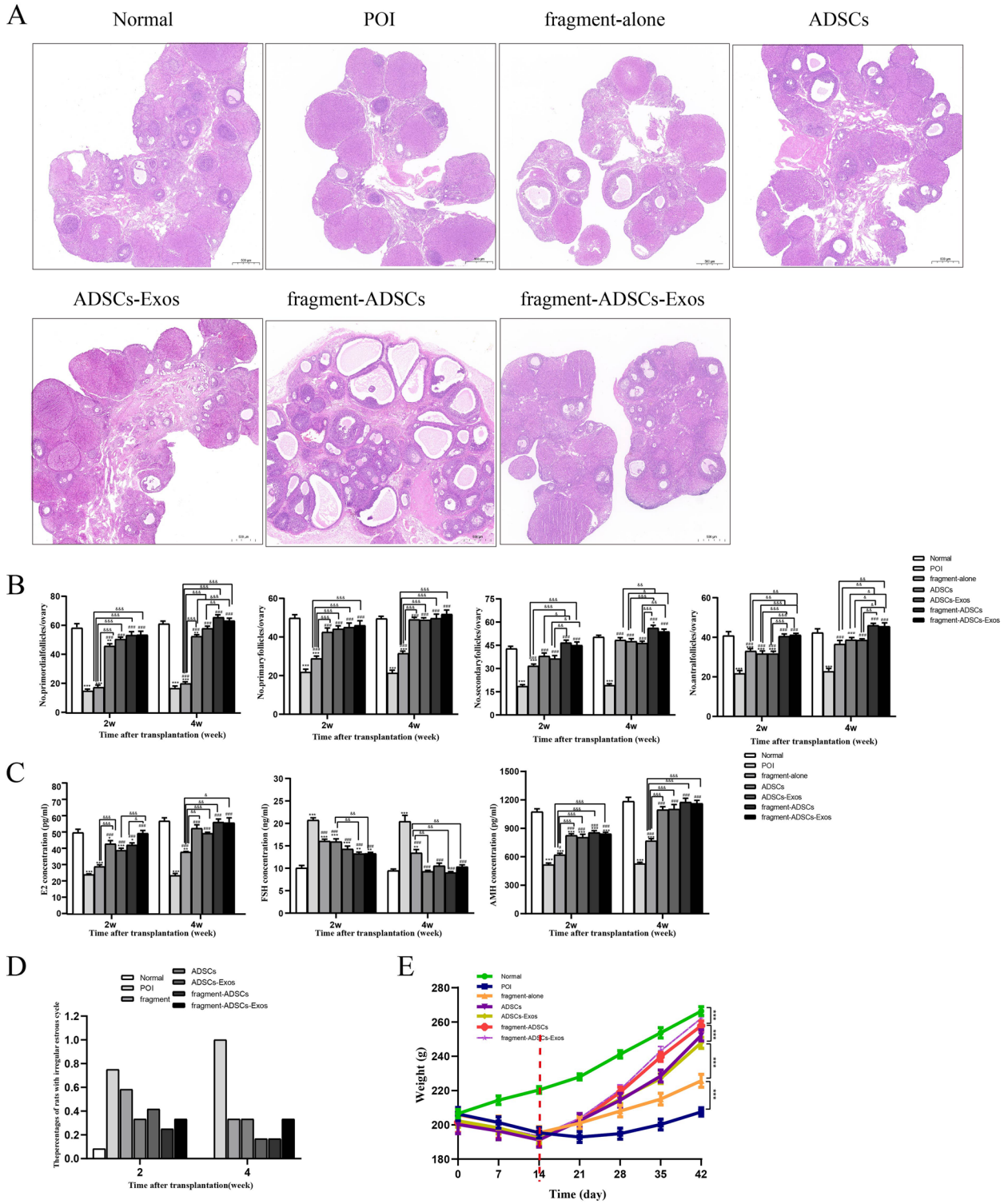

Fig. 2 Changes of ovarian function after transplantation. **A** Histological analysis of ovaries was performed by HE staining. Scale bar: 500 μm. **B** The number of follicles at different developmental stages in each group was counted at 2 and 4 weeks after implantation. Serum levels of E2, FSH, AMH (**C**) and the percentage of irregular estrous cycles (**D**) were evaluated at 2 and 4 weeks after graft transplantation. **E** Changes of body weight were assessed before and after treatment. The red dash line indicates the time points of treatment. (* versus the normal group, # versus the POI group, & comparison between two groups; *, #, & $P < 0.05$; **, ##, && $P < 0.01$; ***, ###, &&& $P < 0.001$; $n = 6$ per group)

in fragment-ADSCs group and ADSCs-treated group, particularly the former, whilst there was no apparent change in the fragment-alone group (Fig. S2B). Likewise, the expression of BCL-2-positive cells was notably up-regulated in fragment-ADSCs group and ADSCs-treated group, while no significant difference was found between the fragment-alone group and POI group (Fig. S2A). Just as evaluated by immunofluorescence, the Cleaved Caspase-3-positive signals in fragment-ADSCs group and ADSCs-treated group were obviously attenuated, as compared with those in POI group and fragment-alone group, especially in the fragment-ADSCs group (Fig. 3A). Although ADSCs-containing treatment decreased apoptosis, the lowest apoptosis signals of TUNEL were still detected in the fragment-ADSCs group (Fig. 3B). Western blot assay of pro-apoptotic proteins Cleaved Caspase-3, Cleaved Caspase-9, Bax and anti-apoptotic protein BCL-2 demonstrated the relatively lower apoptosis in ADSCs-treated group, which further confirmed the anti-apoptotic roles of ADSCs (Fig. 4A).

ADSCs reduced apoptosis of ovarian GCs through a paracrine mechanism

Accumulating studies suggested the key mechanism of action of ADSCs on POI through the paracrine effects; therefore, we further investigated the effects of ADSCs-Exos on ameliorating chemotherapy-induced ovarian damage. Similarly, we examined the expression of apoptosis-related indicators in in vivo animal models with different therapeutic modalities. Immunodetection techniques revealed that the expression of Bax and Cleaved Caspase-3 in fragment-ADSCs-Exos group and ADSCs-Exos-treated group was reduced as compared with POI group and fragment- alone group, especially in fragment-ADSCs-Exos group (Fig. S2B, 3A), which was consistent with results of the TUNEL staining (Fig. 3B). However, the expression of BCL-2 after immunohistochemical staining was increased in ADSCs-Exos-containing treatment groups (Fig. S2A). Western blot analysis was also conducted to investigate the alterations in expression levels of apoptosis-related proteins, and the ADSCs- treated group and ADSCs-Exos-treated group had increased BCL-2 protein level and reduced ratio of Cleaved Caspase-3 to Caspase-3, Bax, and Cleaved Caspase-9 to Caspase-9, while there was no marked difference between groups (Fig. 4A, B). This confirmed that ADSCs-Exos also exerted the same anti-apoptotic effect as ADSCs via the BCL-2 family. For further analysis, we compared the effects of ADSCs-containing treatment group and ADSCs-Exos-containing treatment group on apoptosis. Compared with the POI and fragment-alone groups, there was significantly reduced expression levels of Bax, Cleaved Caspase-3/Caspase-3 and Cleaved Caspase-9 /Caspase-9 protein and increased expression level of BCL-2 in ADSCs-Exos group, fragment-ADSCs group, and fragment-ADSCs-Exos group, but there was no significant difference between these three groups (Fig. 4C, D, $P > 0.05$), which further confirmed that combined treatment had better anti-apoptotic effect than the drug-free IVA alone. The above results suggested that there was considerable improvement in damaged ovarian function after chemotherapy-induced or mechanical damage-induced (ovarian fragmentation) apoptosis in both ADSCs-treated groups and ADSCs-Exos-treated groups. Although the expression of pro-apoptotic proteins was significantly reduced and anti-apoptotic proteins was significantly increased in the combination treatment groups compared with the groups treated with ADSCs or ADSCs-Exos alone, the difference was not statistically significant.

ADSCs-Exos-containing treatment contributed to follicular development and suppressed apoptosis in vitro

Our in vivo animal experiments have confirmed that paracrine mechanism plays a key role in stem cell-mediated therapy. Therefore, we further established in vitro cultured experiments to explore the effect of ADSCs-Exos on ovarian follicular development. The ovaries of 15-day-old rats contain primarily pre-antral follicles and thus it may be best suited to evaluate the follicular development [26]. Ovarian follicles were grouped as previously defined [26, 27]: primordial follicles; primary and secondary follicles were categorized as pre-antral follicles; antral and preovulatory follicles were classified as large growing follicles. As shown in Fig. 5A, the number of pre-antral follicles ($P < 0.001$) and large growing follicles ($P < 0.05$) were significantly facilitated in fragment-alone group; however, the number of primordial follicles ($P < 0.001$) were obviously decreased in the control group. Interestingly, the number of pre-antral follicles ($P < 0.05$) and large growing follicles ($P < 0.001$) in the fragment-low-Exos group and fragment-high-Exos group was greater than that in the control group, while the number of primordial follicles ($P < 0.001$) was greater than that in fragment-alone group, suggesting that fragment-ADSCs-Exos treatment not only promoted follicular development but also prevented the excessive loss of primordial follicles. With extended periods of culture time, the number of primordial follicles was significantly decreased in all groups, especially in the fragment-alone group (Fig. 5B). In the meantime, the number of large growing follicles in fragment-alone group ($P < 0.01$) and ADSCs-Exos-treated groups ($P < 0.05$) was obviously increased in the control group (Fig. 5B).

Next, we assessed the proliferation/apoptosis levels of the follicles in the four groups. As compared with the

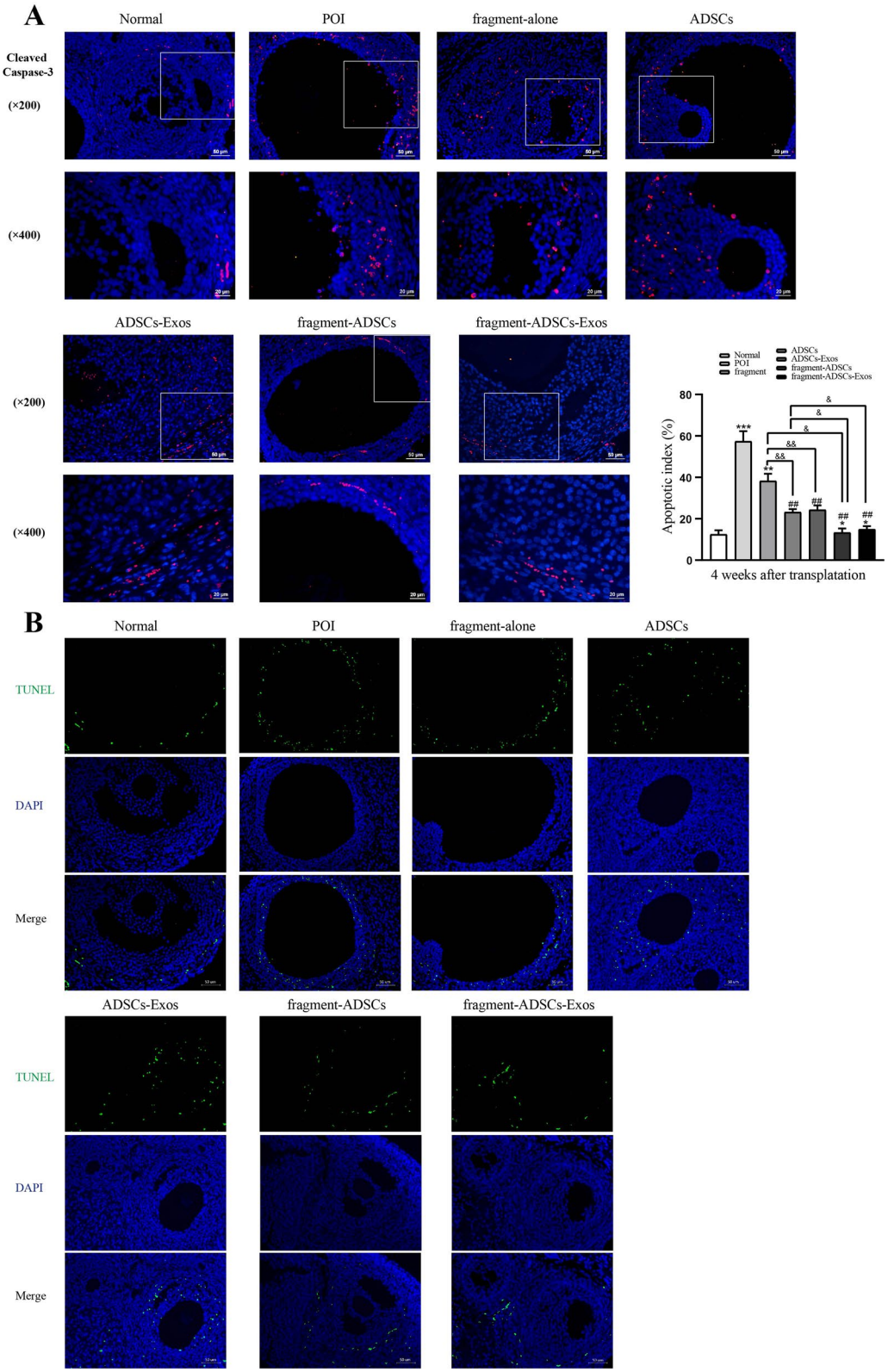

Fig. 3 The effects of graft transplantation on apoptosis of ovarian GCs in POI rats. **A** Representative immunofluorescence staining of Cleaved Caspase-3 in seven different groups. Scale bar: 50 μm and 200 μm. Analysis of the apoptotic index of Cleaved Caspase-3 was conducted using Image-Pro Plus. **B** Representative pictures of TUNEL staining in seven different groups. Scale bar: 50 μm. (* versus the normal group, # versus the POI group, & comparison between two groups; *, #, & $P < 0.05$; **, ##, && $P < 0.01$; ***, ###, &&& $P < 0.001$; $n = 6$ per group)

control group and fragment-alone group, the immunofluorescence intensity of Ki67 was significantly increased in the fragment-low-Exos group ($P<0.01$) and fragment-high-Exos group ($P<0.01$) in the ovaries cultured in vitro for 2 and 4 days (Fig. 6A). Additionally, mechanical damage (ovarian fragmentation) led to increased apoptosis level of Cleaved Caspase-3 in the fragment-alone group (Fig. 6B, $P<0.001$), and the apoptosis level was increased with the prolongation of culture time. However, there was a significant decrease in apoptotic index after treatment in combination with low/high ADSCs-Exos during the whole culture experiment ($P<0.001$). There was no difference in either promoting follicular development or inhibiting cell apoptosis between the fragment-low-Exos and fragment-high-Exos groups ($P>0.05$). All these findings suggested that ovarian fragmentation could activate growth and development of the follicles, which in combination with ADSCs-Exos could control excessive activation of the follicles, promote follicular proliferation and inhibit apoptosis.

Discussion

To our knowledge, this is the first preclinical study to demonstrate that ADSCs-Exos combined with drug-free IVA offers a protective role against chemotherapy-induced ovarian damage through inhibiting apoptosis and that the combination therapy of cell-free bioresource and drug-free IVA may be a promising effective treatment for POI. In the present study, we found that the effect of ADSCs-Exos was comparable to that of ADSCs, and further demonstrated that the combination therapy was superior to ADSCs-Exos alone therapy in promoting follicular development and restoring damaged ovarian function. Short-term in vitro cultures of ovarian fragments and ADSCs-Exos could not only promote follicular development, but also prevent the loss of follicles during the process of ovarian fragmentation and culture, while promoting ovarian cell proliferation and inhibiting apoptosis.

Our prior findings have confirmed that ovarian fragments in conjunction with ADSCs could promote early post-transplantation neovascularization and reduce ischemic injury, thus increasing the survival rate of follicles [13]. Zhai et al. [28] proposed a shortened IVA procedure that reduces follicular apoptosis during ovarian fragmentation by applying large ovarian cortex strips and shortening in vitro culture time, thereby improving the clinical treatment efficiency of IVA. ADSCs-Exos were demonstrated to restore ovarian function in POI mice by inhibiting granulosa cell apoptosis [29]. Likewise, we performed in vivo and in vitro ovarian culture experiments to verify the therapeutic effects of ADSCs-Exos combined with drug-free IVA in repairing the damaged ovarian function of POI rats by inhibiting follicular apoptosis. Our in vitro culture experiment confirmed that the percentage of the pre-antral and large growing follicles increased, accompanied by a decrease in primordial follicles in fragment-alone group, which was consistent with the results of Kawamura et al. [3]. However, low/high Exos combined therapy could not only promote follicular development, but also prevent excessive loss of primordial follicles and improve ovarian reserve. In addition, it can avoid extensive follicular apoptosis caused by ovarian fragment preparation and in vitro culture, promote follicle proliferation and protect these cells from apoptosis.

The results from in vivo experiments showed a reduced ovarian reserve, dysfunctional folliculogenesis, and steroid disorder in POI rat model (Fig. 2). The number of secondary and antral follicles increased in the fragment-alone group, while the number of primordial follicles did not increase, which was attributed to the disruption of Hippo signaling pathway promoting the development of dormant follicles. Although hormone levels and estrous cycles had faster recovery than those in the POI group, the therapeutic effect was far from ideal. Excitingly, in the ADSCs-containing or ADSCs-Exos-containing groups, not only did the number of follicles at all stages of development increase, but also hormone levels and estrous cycle returned to normal, particularly in the fragment-ADSCs/fragment-ADSCs-Exos-treated groups. This might be related to the protective effect of follicles by ADSCs/ADSCs-Exos [30] and the promotion of early graft vascular reconstruction to reduce the ischemic injury of follicles [13], and the combination with ovarian fragments could further promote follicular development and play a better synergistic therapeutic effect.

One of the pathological features of decreased ovarian function is apoptosis. The BCL-2 family exerts an

(See figure on next page.)

Fig. 4 Western blot used to detect the expression of apoptosis-related protein in each group. Protein expression levels of Cleaved Caspase-3, Caspase-3, Cleaved Caspase-9, Caspase-9, Bax and BCL-2 were detected in ADSCs-/ADSCs-Exos-containing-treated groups (**A**) and different treatment groups (**C**). Quantitative analysis of protein expression indicated that the expression level of Cleaved Caspase-3, Cleaved Caspase-9 and Bax was reduced, whereas BCL-2 expression was increased in ADSCs-treated group, ADSCs-Exos-treated group (**B**), fragment-ADSCs group and fragment-ADSCs-Exos group (**D**). (* versus the normal group, # versus the POI group, & comparison between two groups; *, #, & $P<0.05$; **, ##, && $P<0.01$; ***, ###, &&& $P<0.001$; $n=3$ per group)

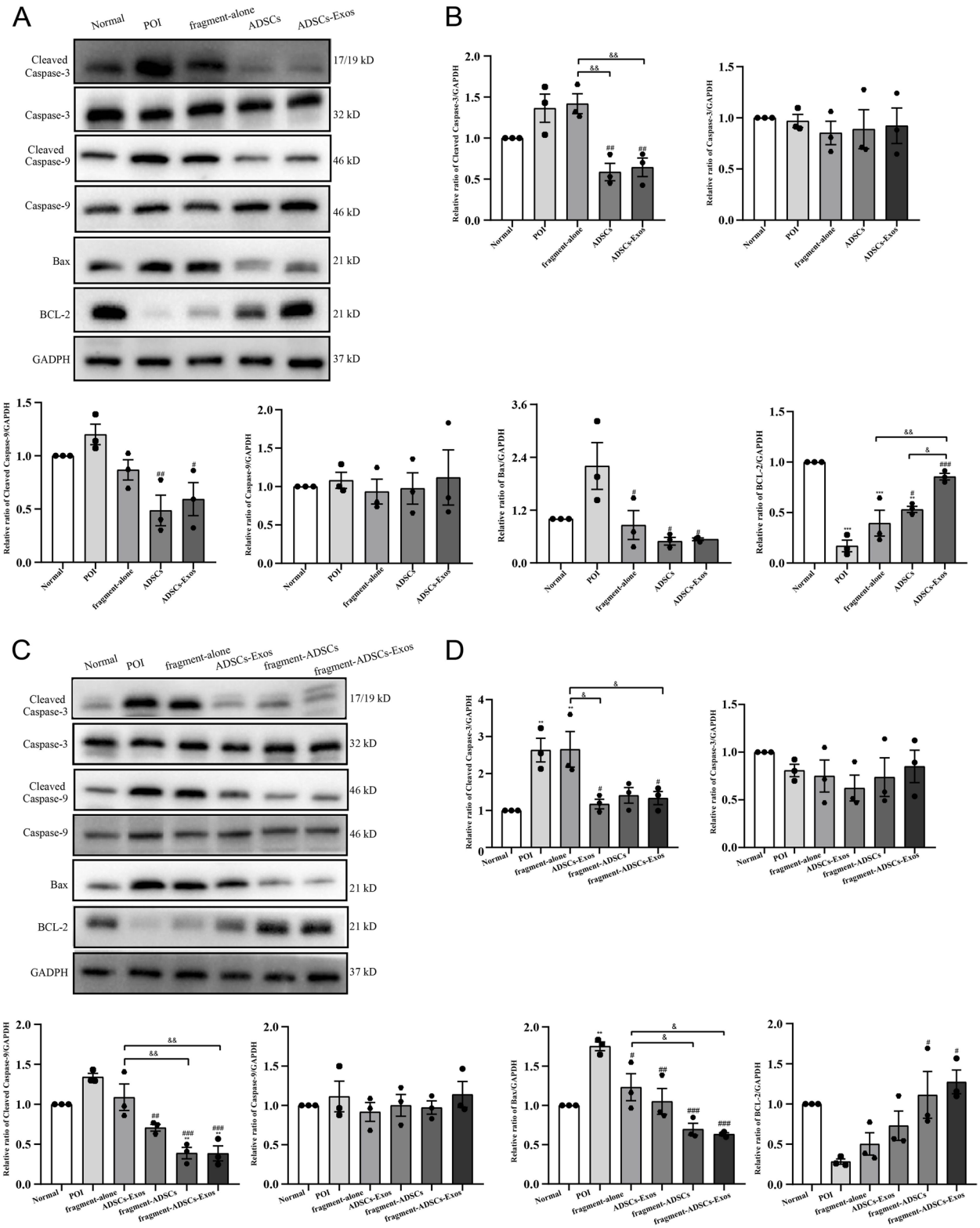

Fig. 4 (See legend on previous page.)

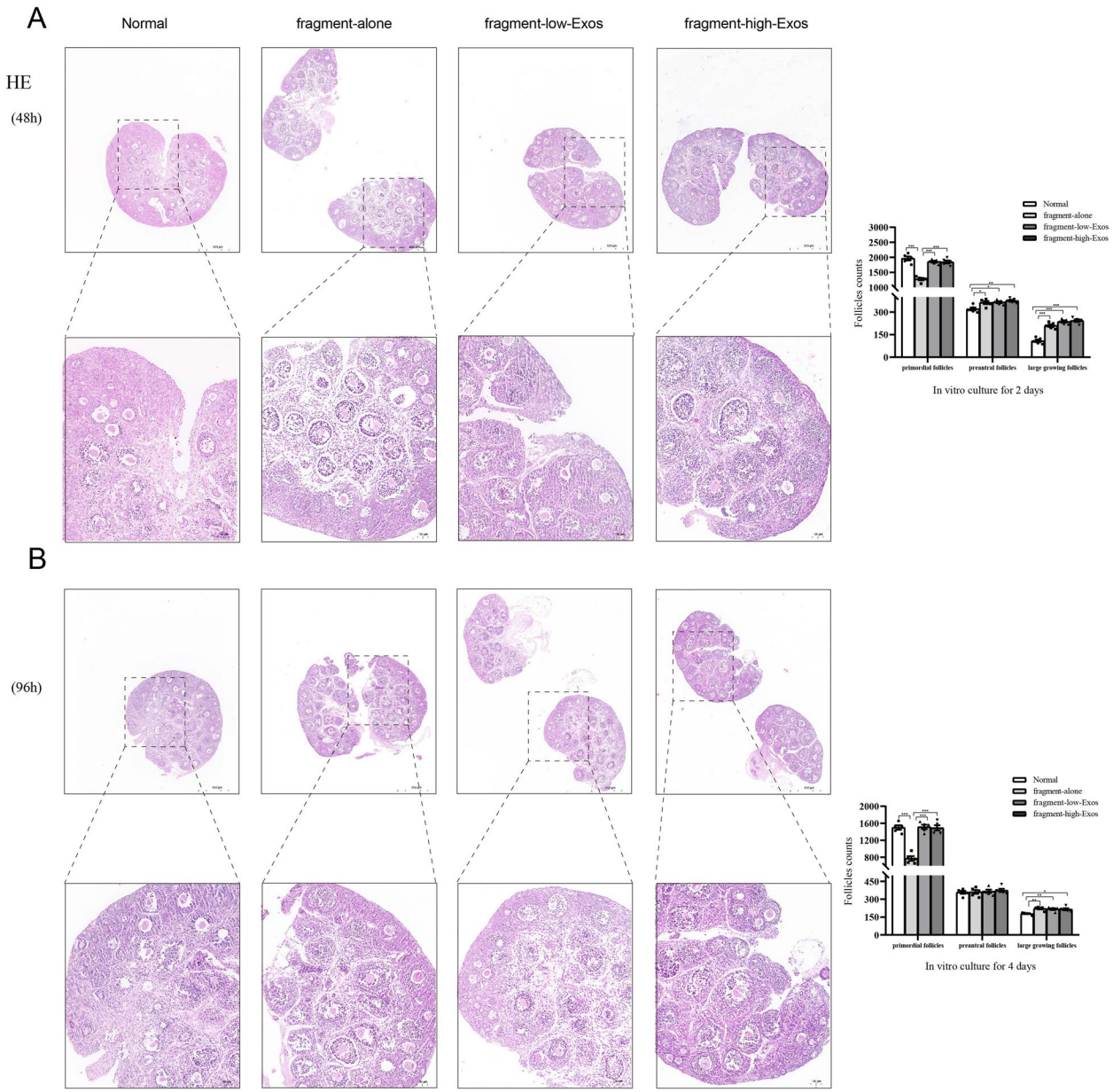

Fig. 5 Ovarian morphology of rat ovaries after in vitro culture. HE staining of ovaries (middle sections) and quantification of the follicles of different types for 48 h (**A**) and 96 h (**B**) in vitro culture. Scale bar: 500 μm and 100 μm. * $P<0.05$, ** $P<0.01$, *** $P<0.001$; $n=5$ per group

important regulatory effect on ovarian cell apoptosis [31]. BCL-2 is an anti-apoptotic protein that prolongs cell survivals [32], while Bax is a pro-apoptotic protein that plays a pivotal role in the process of apoptosis, and its overexpression could accelerate cell apoptosis [33] and potentiate the activation effect of intracellular caspase protease [34]. Of them, Caspase-9 is the initiation molecule of apoptosis, and Caspase-3 is the effector molecule of apoptosis [35], which are important effector molecules in the process of apoptosis. In our study, in comparison with POI group and fragment-alone group, the expression of apoptosis molecules (Bax, Cleaved Caspase-3 and Cleaved Caspase-9) was significantly decreased, whereas the expression of anti-apoptosis molecules (BCL-2) was significantly increased in the ADSCs-containing or ADSCs-Exos-containing groups. Therefore, we speculated that ADSCs might up-regulate BCL-2 expression and down-regulate Bax expression due to the secretion of Exos, thereby reducing the apoptosis of chemotherapy-induced follicle cells, and further promoting the

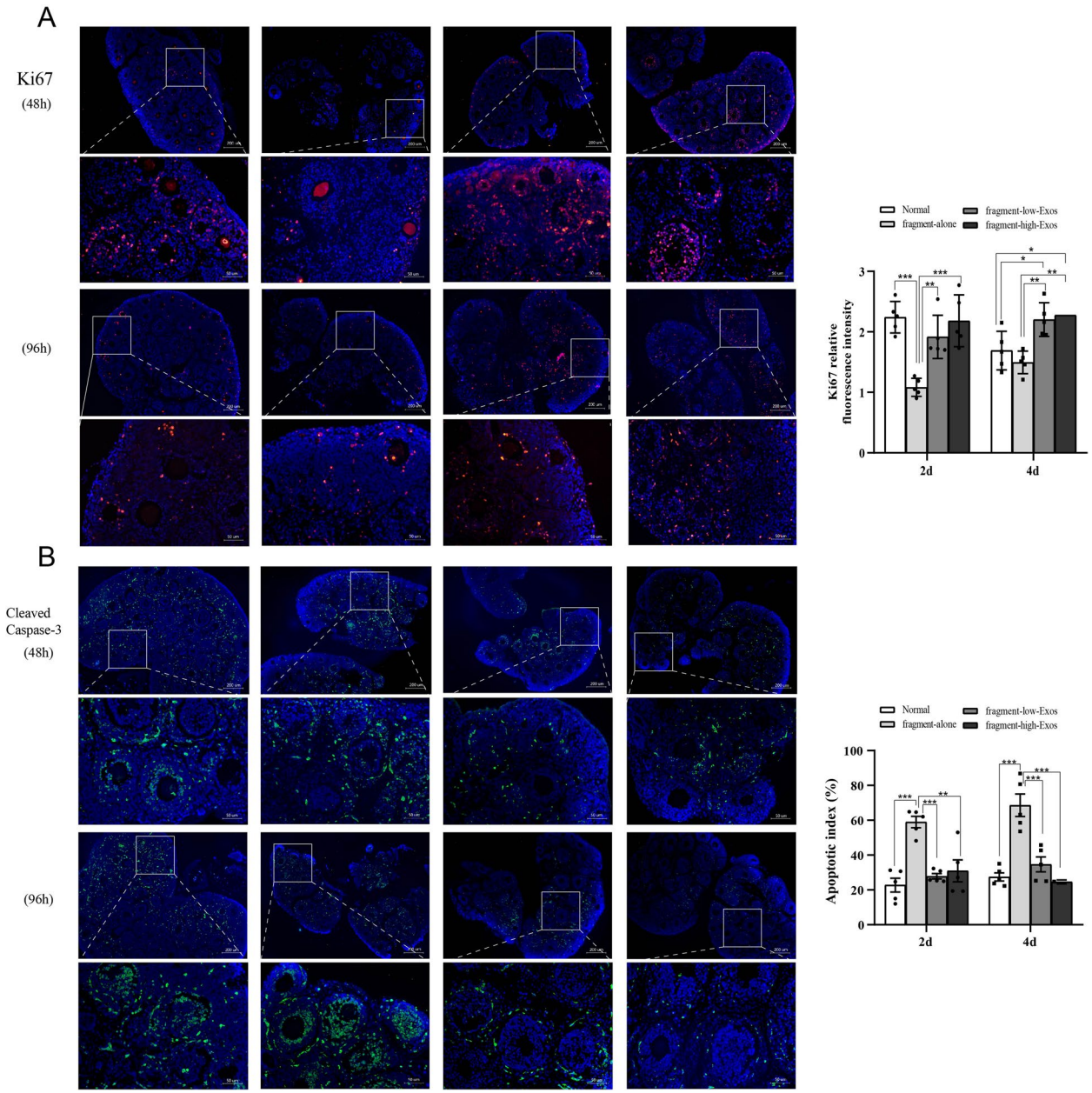

Fig. 6 Follicular proliferation and apoptosis analysis of rat ovaries after in vitro culture. **A** Immunofluorescence of Ki67 in ovaries (red) and statistical analysis of fluorescence intensity. Nuclei were counter-stained with DAPI (blue). **B** Immuno- fluorescence of Cleaved Caspase-3 in ovaries (green) and statistical analysis of apoptotic index. Nuclei were counter-stained with DAPI (blue). Scale bar: 50 μm and 200 μm. * $P < 0.05$, ** $P < 0.01$, *** $P < 0.001$; $n = 5$ per group

development of the follicles and rescue ovarian function in POI-damaged ovary.

In this study, we confirmed the effectiveness of drug-free IVA combined with ADSCs-Exos in restoration of ovarian function of POI, and conducted a preliminary exploration of the anti-apoptotic mechanism. Next, we should further explore the molecular mechanism and its therapeutic effect at different levels to improve its therapeutic efficiency and the therapeutic effectiveness of stem cells from other sources. In addition, we should further explore the effects of ADSCs-Exos on the recovery of oocytes' function and on the interactions between oocytes and granulosa cells. The assessment of fertility was not applied due to tubal adhesion and edema, and there was no standard regimen for the administration of ADSCs and ADSCs-Exos; therefore, we merely

performed the administration based on the exploration of previous experiments and pre-experiments. Thus, relevant studies should be conducted in the future to ameliorate these deficits.

Conclusion

Overall, we confirmed that ADSCs-Exos combined drug-free IVA had a remarkably therapeutic effects in restoring ovarian function of POI rats, and ADSCs-Exos combined treatment was beneficial in promoting follicular development and inhibiting ovarian cell apoptosis in vitro. The paracrine mechanism mediated by ADSCs for restoring chemotherapy-induced ovarian damage might be attributed to the secretion of Exos, which reduced the apoptosis of follicle cells, promoted the development of follicles and rescued ovarian function by up-regulating the expression of BCL-2, and down-regulating the expression of Bax. Taken together, our study has confirmed that ADSCs-Exos and drug-free IVA combination therapy may be a promising treatment for POI.

Abbreviations

Drug-free IVA	Drug-free in vitro activation
POI	Premature ovarian insufficiency
ADSCs	Adipose-derived stem cells
ADSCs-Exos	ADSCs-derived exosomes
MSCs	Mesenchymal stem cells
Exos	Exosome
MSCs-Exos	Exos derived from MSCs
PTEN	Phosphatase and tensin homolog
PI3K	Phosphatidylinositol-3-kinase
GCs	Granulosa cells
TEM	Transmission electron microscopy
NTA	Nanoparticle tracking analysis
OCT	Optimal cutting temperature
HE	Hematoxylin and Eosin
DAPI	4′6-Diamidino-2-Phenylindole
PBS	Phosphate-buffered saline
CTX	Cyclo- phosphamide
IF	Immunofluorescence
ELISA	Enzyme-linked immunosorbent assay
E2	Estradiol
FSH	Follicle stimulating hormone
AMH	Antimüllerian hormone
BSA	Bovine serum albumin
HRT	Hormone replacement therapy

Supplementary Information

The online version contains supplementary material available at https://doi.org/10.1186/s13048-024-01475-4.

Supplementary Material 1: Fig. S1 Procedure of ovarian orthotopic transplantation and characterization and tracing of ADSCs-Exos. (A) Steps of orthotopic transplantation involves injecting saline into the ovarian bursa (a) to separate the oviduct from the ovary as much as possible, removing the ovary (b), and transplanting the ovarian fragments back into the tunnel beneath the ovarian bursa (c). Left figure (d) is the postoperative picture, and right figure (e) is the picture of grafts taken at 4 weeks post-surgery. (B) Representative picture of ADSCs-Exos observed by TEM (scale bar = 200 nm). (C) Size distribution and concentration of ADSCs-Exos by NTA. The mean diameter and particle concentration of ADSCs-Exos were 121.1 nm and 4 × 1011 particles/ml. (D) Western blot showed that in this study ADSCs-Exos were highly positive for CD9, CD63 and TSG101, and negative for GM130. (E) Localization of ADSCs-Exos in rat ovaries. EvLINK555-labeled ADSCs-Exos were primarily distributed in the interstitium of the ovary. The EvLINK555 labeled outer membrane of exosomes was red and the DAPI labeled nucleus was blue. Scale bar:100 μm and 50 μm.

Supplementary Material 2: Fig. S2 Representative immunohistochemical images of BCL-2 (A) and Bax (B) in seven different groups. Scale bar: 50 μm and 200 μm. Analysis of the mean optical density (MOD) of BCL-2-positive/Bax-positive areas were conducted using Image- Pro Plus. (* versus the normal group, # versus the POI group, & comparison between two groups; *, #, & $P < 0.05$; **, ##, && $P < 0.01$; ***, ###, &&& $P < 0.001$; $n = 6$ per group).

Acknowledgements

The authors would like to thank Dr. Yanbiao Song for his technical assistance.

Authors' contributions

Q.L., J.K.Z. and X.H.H. conceived and designed the study, conducted the experiments and wrote the manuscript. Q.L., Z.Q.Z, Z.K.L. and W.X.S. were responsible for data analysis and figure preparation/creation. Z.K.L. and Y.L.X. discussed and revised the manuscript. X.H.H. and Q.L. reviewed the manuscript. All authors have read and approved the final manuscript. Q.L. and X.H.H. has confirmed the authenticity of all the raw data.

Funding

This study was supported by the Chengde City Science and Technology Plan Self-funded Project (202303A173); the Natural Precision Medicine Joint Fund Nurture Project of Hebei Province (H2021206463); the Medical Science Research Plan Project of Hebei Province (20210080); the Innovative Capacity Improvement Plan of Hebei Province (20577705D).

Availability of data and materials

No datasets were generated or analysed during the current study.

Declarations

Ethics approval and consent to participate

The principles outlined in the Declaration of Helsinki and the Guidelines for the Care and Use of Laboratory Animals of the Chinese Institute of Health were strictly adhered to in the present study. The authors also complied with the ARRIVE guidelines. Ethical approval for the animal experiments was obtained from the Ethics Committee of the Affiliated Hospital of Chengde Medical University (CYCYLL 2023713). All animal experiments conducted in the present study followed the guidelines and regulations specified in this ethical approval.

Consent for publication

Not applicable.

Competing interests

The authors declare no competing interests.

Author details

[1]Department of Gynecology, Affiliated Hospital of Chengde Medical University, Chengde, Hebei 067000, P.R. China. [2]Department of Obstetrics and Gynecology, Hebei Key Laboratory of Regenerative Medicine of Obstetrics and Gynecology, The Second Hospital of Hebei Medical University, 215 Heping West Road, Shijiazhuang, Hebei 050000, P.R. China.

Received: 11 March 2024 Accepted: 11 July 2024
Published online: 31 July 2024

References

1. Stuenkel CA, Gompel A. Primary ovarian insufficiency. N Engl J Med. 2023;388(2):154–63. https://doi.org/10.1056/NEJMcp2116488.

2. Kovanci E, Schutt AK. Premature ovarian failure: clinical presentation and treat- ment. Obstet Gynecol Clin North Am. 2015;42(1):153–61. https://doi.org/10.1016/j.ogc.2014.10.004.
3. Kawamura K, Cheng Y, Suzuki N, Deguchi M, Sato Y. Hippo signaling disruption and Akt stimulation of ovarian follicles for infertility treatment. Proc Natl Acad Sci USA. 2013;110(43):17474–9. https://doi.org/10.1073/pnas.1312830110.
4. Kawamura K, Kawamura N, Hsueh AJ. Activation of dormant follicles: a new treatment for premature ovarian failure?. Curr Opin Obstet Gynecol. 2016;28(3):217–22. https://doi.org/10.1097/GCO.0000000000000268.
5. Fabregues F, Ferreri J, Calafell JM, Moreno V, Borrás A, Manau D, et al. Pregnancy after drug-free in vitro activation of follicles and fresh tissue auto- transplantation in primary ovarian insufficiency patient: a case report and literature review. J Ovarian Res. 2018;11(1):76. https://doi.org/10.1186/s13048-018-0447-3.
6. Wang W, Todorov P, Isachenko E, Rahimi G, Mallmann P, Wang M, et al. In vitro activation of cryopreserved ovarian tissue: a single-arm meta-analysis and systematic review. Eur J Obstet Gynecol Reprod Biol. 2021;258:258–64. https://doi.org/10.1016/j.ejogrb.2021.01.014.
7. Halicioglu BS, Saadat KA, Tuglu MI. Adipose-derived mesenchymal stem cell transplantation in chemotherapy-induced premature ovarian insufficiency: the role of connexin and pannexin. Reprod Sci. 2021;29(4):1316–31. https://doi.org/10.1007/s43032-021-00718-9.
8. Salvatore G, Felici MD, Dolci S, Tudisco C, Cicconi R, et al. Human adipose- derived stromal cells transplantation prolongs reproductive lifespan on mouse models of mild and severe premature ovarian insufficiency. Stem Cell Res Ther. 2021;12(1):537. https://doi.org/10.1186/s13287-021-02590-5.
9. Nouri N, Aghebati-Maleki L, Yousefi M. Adipose-derived mesenchymal stem cells: a promising tool in the treatment of pre mature ovarian failure. J Reprod Immunol. 2021;147. https://doi.org/10.1016/j.jri.2021.103363.
10. Hoang VT, Nguyen HP, Nguyen VN, Hoang DM, Nguyen TS, et al. Adipose-derived mesenchymal stem cell therapy for the management of female sexual dysfunction: Literature reviews and study design of a clinical trial. Front Cell Dev Biol. 2022;28(10). https://doi.org/10.3389/fcell.2022.956274.
11. Green LJ, Zhou H, Padmanabhan V, Shikanov A. Adipose-derived stem cells promote survival, growth, and maturation of early-stage murine follicles. Stem Cell Res Ther. 2019;10(1):10. https://doi.org/1186/s13287-019-1199-8.
12. Ai G, Meng M, Guo J, Li C, Zhu J, et al. Adipose-derived stem cells promote the repair of chemotherapy-induced premature ovarian failure by inhibiting granulosa cells apoptosis and senescence. Stem Cell Res Ther. 2023;14(1):10. https://doi.org/1186/s13287-023-03297-5.
13. Li Q, Zheng J, Li Z, Xiao Y, Zhang M, et al. Drug-free in vitro activation combined with 3D-bioprinted adipose-derived stem cells restores ovarian function of rats with premature ovarian insufficiency. Stem Cell Res Ther. 2022;13(1):347. https://doi.org/10.1186/s13287-022-03035-3.
14. Matsuzaka Y, Yashiro R. Therapeutic Strategy of Mesenchymal-Stem-Cell-Derived Extracellular Vesicles as Regenerative Medicine. Int J Mol Sci. 2022;23(12):6480. https://doi.org/10.3390/ijms23126480.
15. Liao Z, Liu C, Wang L, Sui C, Zhang H. Therapeutic Role of Mesenchymal Stem Cell-Derived Extracellular Vesicles in Female Reproductive Diseases. Front Endocrinol (Lausanne). 2021;23(12).
16. Sajeesh S, Broekelman T, Mecham RP, Ramamurthi A. Stem cell derived extracellular vesicles for vascular elastic matrix regenerative repair. Acta Biomater. 2020;113:267–78. https://doi.org/10.1016/j.actbio.2020.07.002.
17. Xu S, Liu C, Ji HL. Concise review: therapeutic potential of the mesenchymal stem cell derived secretome and extracellular vesicles for radiation-induced lung injury: progress and hypotheses. Stem Cells Transl Med. 2019;8(4):344–54. https://doi.org/10.1002/sctm.18-0038.
18. Boyiadzis M, Whiteside TL. The emerging roles of tumor-derived exosomes in hematological malignancies. Leukemia. 2017;31(6):1259–68. https://doi.org/10.1038/leu.2017.91.
19. Valadi H, Ekstrom K, Bossios A, Sjostrand M, Lee JJ, Lotvall JO. Exosome-mediated transfer of mRNAs and microRNAs is a novel mechanism of genetic exchange between cells. Nat Cell Biol. 2007;9(6):654–9. https://doi.org/10.1038/ncb1596.
20. Ren Y, He J, Wang X, Liang H, Ma Y. Exosomes from adipose-derived stem cells alleviate premature ovarian failure via blockage of autophagy and AMPK/mTOR pathway. PeerJ. 2023;14(11). https://doi.org/10.7717/peerj.16517.
21. Weng Z, Zhang B, Wu C, Yu F, Han B, et al. Therapeutic roles of mesenchymal stem cell-derived extracellular vesicles in cancer. J Hematol Oncol. 2021;14(1):10. https://doi.org/1186/s13045-021-01141-y.
22. Pluchino S, Smith JA. Explicating exosomes: reclassifying the rising stars of intercellular communication. Cell. 2019;177(2):225–7. https://doi.org/10.1016/j.cell.2019.03.020.
23. Yaghoubi Y, Movassaghpour A, Zamani M, Talebi M, Mehdizadeh A, Yousefi M. Human umbilical cord mesenchymal stem cells derived-exosomes in diseases treatment. Life Sci. 2019;233:116733. https://doi.org/10.1016/j.lfs.2019.116733.
24. Zhao SD, Qi WB, Zheng JH, Tian YP, Qi XJ, Kong DS, et al. Exosomes derived from adipose mesenchymal stem cells restore functional endometrium in a rat model of intrauterine adhesions. Reprod Sci. 2020;27(6):1266–75. https://doi.org/10.1007/s43032-019-00112-6.
25. Li Z, Zhang M, Zheng J, Tian Y, Zhang H, Tan Y, et al. Human umbilical cord mesenchymal stem cell-derived exosomes improve ovarian function and proliferation of premature ovarian insufficiency by regulating the hippo signaling pathway. Front Endocrinol (Lausanne). 2021;12:711902. https://doi.org/10.3389/fendo.2021.711902.
26. Qin X, Zhao Y, Zhang T, Yin C, Qiao J, Guo W, et al. TrkB agonist antibody ameliorates fertility deficits in aged and cyclophosphamide-induced premature ovarian failure model mice. Nat Commun. 2022;13(1):914. https://doi.org/10.1038/s41467-022-28611-2.
27. Kalich-Philosoph L, Roness H, Carmely A, Fishel-Bartal M, Ligumsky H, Paglin S, et al. Cyclophosphamide triggers follicle activation and "burnout"; AS101 prevents follicle loss and preserves fertility. Sci Transl Med. 2013;5(185):185ra62. https://doi.org/10.1126/scitranslmed.3005402.
28. Zhai J, Yao G, Dong F, Bu Z, Cheng Y, Sato Y, et al. In vitro activation of follicles and fresh tissue auto-transpla- ntation in primary ovarian insufficiency patients. J Clin Endocrinol Metab. 2016;101(11):4405–12. https://doi.org/10.1210/jc.2016-1589.
29. Huang B, Lu J, Ding C, Zou Q, Wang W, Li H. Exosomes derived from human adipose mesenchymal stem cells improve ovary function of premature ovarian insufficiency by targeting SMAD. Stem Cell Res Ther. 2018;9(1):216. https://doi.org/10.1186/s13287-018-0953-7.
30. Yang W, Zhang J, Xu B, He Y, Liu W, Li J, et al. HucMSC- derived exosomes mitigate the age-related retardation of fertility in female mice. Mol Ther. 2020;28(4):1200–13. https://doi.org/10.1016/j.ymthe.2020.02.003.
31. Valentini E, Martile MD, Brignone M, Caprio MD, Manni I, et al. Bcl-2 family inhibitors sensitize human cancer models to therapy. Cell Death Dis. 2023;14(7):441. https://doi.org/10.1038/s41419-023-05963-1.
32. Lee YG, Guruprasad P, Ghilardi G, Pajarillo R, Sauter CT, et al. Modulation of BCL-2 in both T cells and tumor cells to enhance chimeric antigen receptor T-cell immunotherapy against cancer. Cancer Discov. 2022;12(10):2372–91. https://doi.org/10.1158/2159-8290.cd-21-1026.
33. Cosentino K, Hertlein V, Jenner A, Dellmann T, Gojkovic M, et al. The interplay between BAX and BAK tunes apoptotic pore growth to control mitochondrial-DNA -mediated inflammation. Mol Cell. 2022;82(5):933–49. https://doi.org/10.1016/j.molcel.2022.01.008.
34. Wang Q, Zhang L, Yuan X, Ou Y, Zhu X, et al. The relationship between the Bcl-2/Bax proteins and the mitochondria-mediated apoptosis pathway in the differentiation of adipose-derived stromal cells into neurons. PLoS ONE. 2016;11(10):e0163327. https://doi.org/10.1371/journal.pone.0163327.
35. Unnisa A, Greig NH, Kamal MA. Inhibition of Caspase 3 and Caspase 9 mediated apoptosis: a multimodal therapeutic target in traumatic brain injury. Curr Neuropharmacol. 2023;21(4):1001–12. https://doi.org/10.2174/1570159X20666220327222921.

Publisher's Note